

TABLE I. Summary of the Patients With Severe Lipodystrophy and Progeroid Appearance and Mutations in Exon 64 of *FBN1*

	Patient 1, Graul-Neumann et al. [2010]	Patient 2, Goldblatt et al. [2011]	Patient 3, Horn and Robinson [2011]	Patient 4, the propositus	Phenotypic range among Patients 1–4	MFS <sup>a</sup>	SGS <sup>a</sup>	LDS <sup>b</sup>
Age reported/sex	25-year-old/female	20-year-old/male	3.5-year-old/female	10-year-old/female				
Gestational age	36 weeks	28 weeks	32 weeks	34 weeks	Range: 28–36 weeks			
Birth weight	1,780 g [–2.31 SD]	1.04 kg	1,185 g [–1.5 SD]	1,427 g [–2.3 SD]	Below –1.5 SD			
Mutation	c.8155_8156delAA	c.8156_8175del	c.8226+1G>T [IVS64+1G>T]	c.8175_8182del8bp	Exon/intron 64 of <i>FBN1</i>	<i>FBN1</i>	<i>SKI</i>	<i>TGFBR1/2</i>
Amino acids	p.Lys2719AspfsX18	p.Lys2719ThrfsX12	Splice site	p.Arg2726Glufs*9	“ETEKHKRN” motif at carboxyl terminus			
Congenital lipodystrophy	Present	Present	Present	Present	4/4	–	–	–
Extreme thinness (body mass index)	Present (13.3 kg/m <sup>2</sup> at 25-year-old)	Present (NR)	Present (12.4 kg/m <sup>2</sup> at 2-year-old)	Present (9.8 kg/m <sup>2</sup> at 10-year-old)	4/4	+	–	–
Arachnodactyly	Present	Present	Present	Present	4/4	+	+	+
Digital hyper-extensibility	Present	Present	NR	Present	3/4	+	+	+
Progeroid appearance	Present	Present	Present	Present	4/4	–	–	–
Retrognathia	Present	Present	Present	Present	4/4	–	+	+
Prominent forehead/scaphocephaly	NR	NR	Present	Present	2/4	–	+	–
Downslanting palpebral fissures	NR	Present	Present	Present	3/4	+	+	–
Craniosynostosis	NR	NR	NR	Present	1/4	–	+	+
Ectopia lentis	Present	Present	Absent	Absent	3/4	+	–	+
Proptosis	Present	Present	Present	Present	4/4	–	+	–
Severe myopia	Present	Present	Absent	Present	3/4	+	–	–
Cardiovascular complications	Dilatation of the aortic bulb and mild mitral prolapse	Absent	Mild mitral valve prolapse	Absent	2/4	+	–	+
Normal psychomotor development	Present	Present	Present	Present	4/4	+	–	+
Arrested hydrocephalus	NR	Present	Present	Present	3/4	–	+	–
Dural ectasia	Present	NR	NR	Present	2/4	+	–	–
Renal/genitourinary complications	NR	Absent	NR	Hydronephrosis	1/4	–	–	–
Hypertension	NR	NR	NR	Present	1/4	–	–	–

LDS, Loeys–Dietz syndrome; MFS, Marfan syndrome; SGS, Shprintzen–Goldberg syndrome; NR, not recorded. Presence/absence of each phenotype was based on descriptions in <sup>a</sup>Jones [2006] and <sup>b</sup>Loeys et al. [2006].

propositus with the presumably new disease entity suggests that craniosynostosis might be a phenotypic component extending across various disorders that is caused by an aberrant FBN1-TGF beta signaling cascade.

Congenital lipodystrophy and a progeroid appearance are distinctive phenotypes among FBN1-TGF beta signaling disorders. However, it remains unclear whether these additional phenotypes represent a neomorphic mutation or the most severe end of the FBN1-TGF beta signaling spectrum. From a molecular standpoint, we tend to think that they represent a neomorphic mutation. The four progeroid patients had mutations in exon 64 of *FBN1*. Although no apparent genotype–phenotype relationship is known to exist between *FBN1* mutations and Marfan syndrome phenotypes, except for neonatal Marfan syndrome [Kainulainen et al., 1994], a clear genotype–phenotype relationship seems to exist in the four progeroid patients. One hypothetical mechanism would be a defective nonsense-mediated mRNA decay (NMD) triggered by a truncating mutation involving the most carboxyl terminus of the *FBN1* gene. In general, transcripts containing a premature termination codon trigger NMD, leading to mRNA decay or degradation. An exception to this rule is that transcripts with premature termination codons in the last exon and 50–55 bp of the penultimate exon are translated into truncated proteins [Khajavi et al., 2006]. Indeed, the four progeroid patients all had mutations near the 3' end of the penultimate exon, i.e., exon 64, and their protein products likely

escaped from NMD (Fig. 3). Moreover, the functional domain sequence encoded by exons 44–49 of *FBN1*, which releases endogenous TGF beta and stimulates downstream TGF beta receptor signaling [Chaudhry et al., 2007], would have been preserved in the four progeroid patients.

Although this hypothetical explanation seems plausible for the four progeroid patients with a mutation in exon 64, NMD fails to explain other patients with truncating mutations in exon 64 or 65 of *FBN1* who did not present with a progeroid appearance or severe lipodystrophy [Collod-Beroud et al., 1998; Palz et al., 2000; Rommel et al., 2005]. Hence, an additional mechanism in conjunction with NMD is needed to explain the presumed genotype–phenotype relationship by which the penultimate exon causes this specific phenotype. The presence of the “ETEKHKRN” protein motif in the carboxyl termini of the truncated transcripts may be associated with this unique phenotype (Fig. 3). Goldblatt et al. [2011] pointed out that the presence of an extremely charged protein sequence in the carboxyl terminus of the truncated transcripts may affect downstream protein–protein interactions. The observation that the above-mentioned patients with frame-shift mutations in exons 64–65 without progeroid phenotype lacked this “ETEKHKRN” protein motif further augments our hypothesis. These lines of evidence points to the interpretation that this new progeroid syndrome represents a neomorphic phenotype caused by truncated transcripts with an extremely charged protein motif that escape

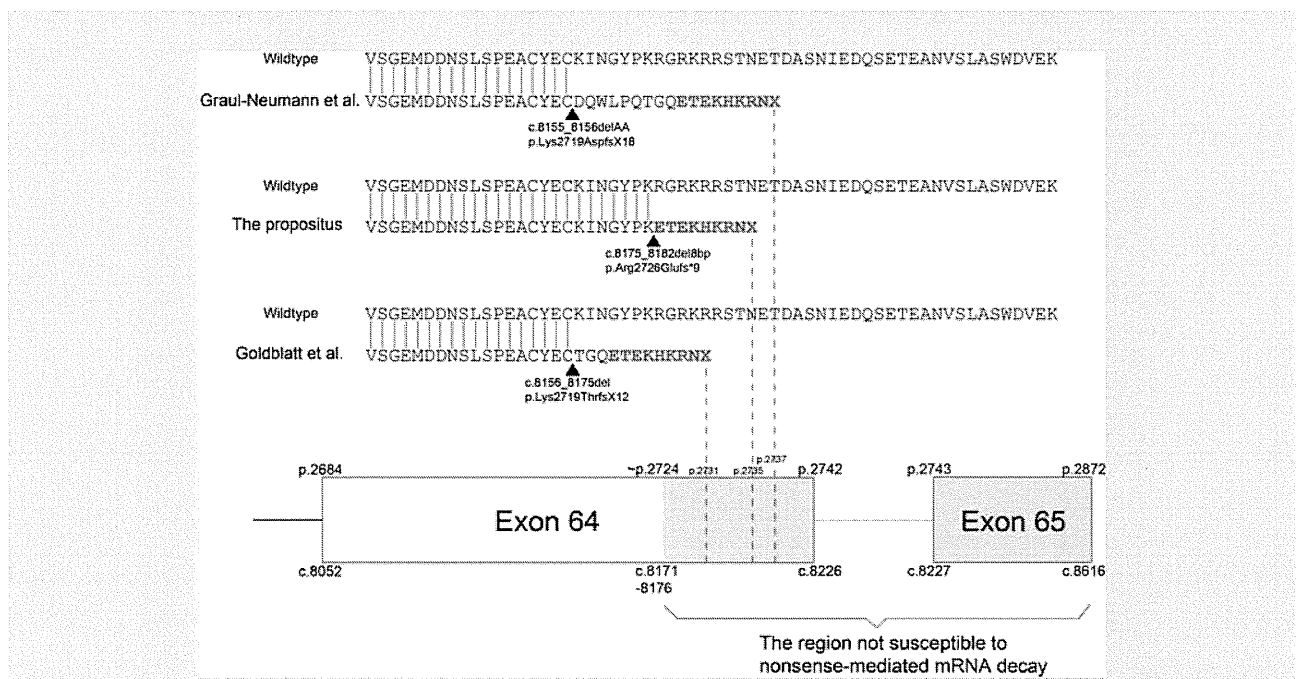


FIG. 3. Common aberrant motif caused by frame-shift mutations in progeroid patients. Predicted protein sequences are shown for the patients reported by Graul-Neumann et al., Goldblatt et al. and the propositus [wildtype, above; patient, below]. Note that all three patients had the same specific protein motif, “ETEKHKRN [in red],” at the carboxyl termini of the transcripts. The black triangles indicate the relative positions of the mutations. The dotted lines indicate the relative positions of the protein truncation on exon 64. The gray area in exons 64 and 65 indicates the genetic region where the truncating mutations are assumed not to trigger nonsense-mediated mRNA decay.

from nonsense-mediated mRNA decay, thereby altering FBN1-TGF beta signaling, rather than the severe end of the phenotypic spectrum of the FBN1-TGF beta signaling disorders.

In conclusion, marfanoid-progeroid syndrome should be included in the differential diagnosis of progeroid syndromes. The diagnostic clues to this new entity are a progeroid appearance accompanied by characteristic growth patterns: premature birth with accelerated height growth that cross growth chart channels and a discrepant poor weight gain, resulting in a severely reduced body mass index. This phenotypic combination should prompt a mutation analysis of the penultimate exon of *FBN1*.

## ACKNOWLEDGMENTS

This work was supported by Research on Applying Health Technology (H23-013) from the Ministry of Health, Labour and Welfare, Japan. We thank Dr. Suketaka Momoshima for insightful discussion on the three-dimensional imaging and Ms. Namiko Saito and Ms. Yumi Obayashi for their technical assistance in article preparation.

## REFERENCES

- Carmignac V, Thevenon J, Ades L, Callewaert B, Julia S, Thauvin-Robinet C, Gueneau L, Courcet JB, Lopez E, Holman K, Renard M, Plauchu H, Plessis G, De Backer J, Child A, Arno G, Duplomb L, Callier P, Aral B, Vabres P, Gigot N, Arbustini E, Grasso M, Robinson PN, Goizet C, Baumann C, Di Rocco M, Sanchez Del Pozo J, Huet F, Jondeau G, Collod-Beroud G, Beroud C, Amiel J, Cormier-Daire V, Riviere JB, Boileau C, De Paepe A, Faivre L. 2012. In-frame mutations in exon 1 of *SKI* cause dominant Shprintzen-Goldberg syndrome. *Am J Hum Genet* 91:950–957.
- Chaudhry SS, Cain SA, Morgan A, Dallas SL, Shuttleworth CA, Kielty CM. 2007. Fibrillin-1 regulates the bioavailability of TGFbeta1. *J Cell Biol* 176:355–367.
- Collod-Beroud G, Beroud C, Ades L, Black C, Boxer M, Brock DJ, Holman KJ, de Paepe A, Francke U, Grau U, Hayward C, Klein HG, Liu W, Nuytinck L, Peltonen L, Alvarez Perez AB, Rantamaki T, Junien C, Boileau C. 1998. Marfan database (third edition): New mutations and new routines for the software. *Nucleic Acids Res* 26:229–233.
- Doyle AJ, Doyle JJ, Bessling SL, Maragh S, Lindsay ME, Schepers D, Gillis E, Mortier G, Homfray T, Sauls K, Norris RA, Huso ND, Leahy D, Mohr DW, Caulfield MJ, Scott AF, Destree A, Hennekam RC, Arn PH, Curry CJ, Van Laer L, McCallion AS, Loeyls BL, Dietz HC. 2012. Mutations in the TGF-beta repressor *SKI* cause Shprintzen-Goldberg syndrome with aortic aneurysm. *Nat Genet* 44:1249–1254.
- Goldblatt J, Hyatt J, Edwards C, Walpole I. 2011. Further evidence for a marfanoid syndrome with neonatal progeroid features and severe generalized lipodystrophy due to frameshift mutations near the 3' end of the *FBN1* gene. *Am J Med Genet Part A* 155A:717–720.
- Graul-Neumann LM, Kienitz T, Robinson PN, Baasanjav S, Karow B, Gillessen-Kaesbach G, Fahsold R, Schmidt H, Hoffmann K, Passarge E. 2010. Marfan syndrome with neonatal progeroid syndrome-like lipodystrophy associated with a novel frameshift mutation at the 3' terminus of the *FBN1*-gene. *Am J Med Genet Part A* 152A:2749–2755.
- Horn D, Robinson PN. 2011. Progeroid facial features and lipodystrophy associated with a novel splice site mutation in the final intron of the *FBN1* gene. *Am J Med Genet Part A* 155A:721–724.
- Inokuchi M, Matsuo N, Anzo M, Hasegawa T. 2007. Body mass index reference values (mean and SD) for Japanese children. *Acta Paediatr* 96:1674–1676.
- Jones KL. 2006. *Smith's recognizable patterns of human malformation*. Philadelphia, PA: Elsevier, Saunders.
- Kainulainen K, Karttunen L, Puhakka L, Sakai L, Peltonen L. 1994. Mutations in the fibrillin gene responsible for dominant ectopia lentis and neonatal Marfan syndrome. *Nat Genet* 6:64–69.
- Khajavi M, Inoue K, Lupski JR. 2006. Nonsense-mediated mRNA decay modulates clinical outcome of genetic disease. *Eur J Hum Genet* 14:1074–1081.
- Kosaki K, Takahashi D, Udaka T, Kosaki R, Matsumoto M, Ibe S, Isoe T, Tanaka Y, Takahashi T. 2006. Molecular pathology of Shprintzen-Goldberg syndrome. *Am J Med Genet Part A* 140:104–108, author reply 109–110.
- Loeyls BL, Schwarze U, Holm T, Callewaert BL, Thomas GH, Pannu H, De Backer JF, Oswald GL, Symoens S, Manouvrier S, Roberts AE, Faravelli F, Greco MA, Pyeritz RE, Milewicz DM, Coucke PJ, Cameron DE, Braverman AC, Byers PH, De Paepe AM, Dietz HC. 2006. Aneurysm syndromes caused by mutations in the TGF-beta receptor. *N Engl J Med* 355:788–798.
- Palz M, Tiecke F, Booms P, Goldner B, Rosenberg T, Fuchs J, Skovby F, Schumacher H, Kaufmann UC, von Kodolitsch Y, Nienaber CA, Leitner C, Katzke S, Vetter B, Hagemeyer C, Robinson PN. 2000. Clustering of mutations associated with mild Marfan-like phenotypes in the 3' region of *FBN1* suggests a potential genotype-phenotype correlation. *Am J Med Genet* 91:212–221.
- Rommel K, Karck M, Haverich A, von Kodolitsch Y, Rybczynski M, Muller G, Singh KK, Schmidtke J, Arslan-Kirchner M. 2005. Identification of 29 novel and nine recurrent fibrillin-1 (*FBN1*) mutations and genotype-phenotype correlations in 76 patients with Marfan syndrome. *Hum Mutat* 26:529–539.
- Tsuzaki S, Matsuo N, Osano M. 1987. The physical growth of Japanese children from birth to 18 years of age. Cross-sectional percentile growth curve for height and weight. *Helv Paediatr Acta* 42:111–119.

## Mutations in *SERPINB7*, Encoding a Member of the Serine Protease Inhibitor Superfamily, Cause Nagashima-type Palmoplantar Keratosis

Akiharu Kubo,<sup>1,2,3,\*</sup> Aiko Shiohama,<sup>1,4</sup> Takashi Sasaki,<sup>1,2,3</sup> Kazuhiko Nakabayashi,<sup>5</sup> Hiroshi Kawasaki,<sup>1</sup> Toru Atsugi,<sup>1,6</sup> Showbu Sato,<sup>1</sup> Atsushi Shimizu,<sup>7</sup> Shuji Mikami,<sup>8</sup> Hideaki Tanizaki,<sup>9</sup> Masaki Uchiyama,<sup>10</sup> Tatsuo Maeda,<sup>10</sup> Taisuke Ito,<sup>11</sup> Jun-ichi Sakabe,<sup>11</sup> Toshio Heike,<sup>12</sup> Torayuki Okuyama,<sup>13</sup> Rika Kosaki,<sup>14</sup> Kenjiro Kosaki,<sup>15</sup> Jun Kudoh,<sup>16</sup> Kenichiro Hata,<sup>5</sup> Akihiro Umezawa,<sup>17</sup> Yoshiki Tokura,<sup>11</sup> Akira Ishiko,<sup>18</sup> Hironori Niizeki,<sup>19</sup> Kenji Kabashima,<sup>9</sup> Yoshihiko Mitsuhashi,<sup>10</sup> and Masayuki Amagai<sup>1,2,4</sup>

“Nagashima-type” palmoplantar keratosis (NPPK) is an autosomal recessive nonsyndromic diffuse palmoplantar keratosis characterized by well-demarcated diffuse hyperkeratosis with redness, expanding on to the dorsal surfaces of the palms and feet and the Achilles tendon area. Hyperkeratosis in NPPK is mild and nonprogressive, differentiating NPPK clinically from Mal de Meleda. We performed whole-exome and/or Sanger sequencing analyses of 13 unrelated NPPK individuals and identified biallelic putative loss-of-function mutations in *SERPINB7*, which encodes a cytoplasmic member of the serine protease inhibitor superfamily. We identified a major causative mutation of c.796C>T (p.Arg266\*) as a founder mutation in Japanese and Chinese populations. *SERPINB7* was specifically present in the cytoplasm of the stratum granulosum and the stratum corneum (SC) of the epidermis. All of the identified mutants are predicted to cause premature termination upstream of the reactive site, which inhibits the proteases, suggesting a complete loss of the protease inhibitory activity of *SERPINB7* in NPPK skin. On exposure of NPPK lesional skin to water, we observed a whitish spongy change in the SC, suggesting enhanced water permeation into the SC due to overactivation of proteases and a resultant loss of integrity of the SC structure. These findings provide an important framework for developing pathogenesis-based therapies for NPPK.

The congenital palmoplantar keratoses (PPKs) are a heterogeneous group of diseases. Phenotypic classification of hereditary PPKs is based mainly on the specific morphology and distribution of the hyperkeratosis, the presence or absence of associated features, and the inheritance pattern and is assisted by additional criteria such as the presence of skin lesions in areas other than the palms and soles, the age at onset of the hyperkeratosis, the severity of the disease process, and histopathological findings.<sup>1</sup>

“Keratosis palmoplantaris Nagashima”<sup>2</sup> or “Nagashima-type” PPK (NPPK)<sup>3</sup> has been proposed as a clinical entity included within the diffuse hereditary PPKs without associated features.<sup>1</sup> A familial case of two siblings was first reported as a distinct clinical type of PPK in 1989.<sup>2,4</sup> Because Nagashima briefly described this type of hereditary PPK in the Japanese literature in 1977,<sup>5</sup> the name “keratosis palmoplantaris Nagashima” was proposed.<sup>2</sup> Although about 20 cases of Japanese individuals with NPPK have been reported in the Japanese literature since then, this clinical

entity was not described in detail in the English language literature until 2008.<sup>3</sup>

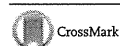
An autosomal recessive trait has been suggested in NPPK.<sup>2,3</sup> The clinical features of NPPK are characterized by well-demarcated reddish and diffuse palmoplantar hyperkeratosis that extends to the dorsal surfaces of the hands, feet, inner wrists, ankles, and the Achilles tendon area.<sup>2–6</sup> Involvement of the elbows and knees and high frequencies of hyperhidrosis on palms and soles have been noted.<sup>3</sup> Clinical observations revealed no differences between males and females, no seasonal change, and no association with squamous cell carcinoma or any other malignancy. Although mild T cell infiltration in the affected skin area has been reported,<sup>7</sup> the pathophysiology of the skin redness and hyperkeratosis are still uncharacterized.

An autosomal recessive trait, transgressive diffuse hyperkeratosis, and the absence of associated features are also characteristic of Mal de Meleda (MDM [MIM 248300]),<sup>8</sup> PPK Gamborg Nielsen (Norrboten recessive type PPK [MIM 244850]),<sup>9,10</sup> and acral keratoderma.<sup>11</sup> These other

<sup>1</sup>Department of Dermatology, Keio University School of Medicine, Tokyo 160-8582, Japan; <sup>2</sup>Keio-Maruho Laboratory of Skin Barriology, Keio University School of Medicine, Tokyo 160-8582, Japan; <sup>3</sup>Center for Integrated Medical Research, Keio University School of Medicine, Tokyo 160-8582, Japan; <sup>4</sup>MSD Endowed Program for Allergy Research, Keio University School of Medicine, Tokyo 160-8582, Japan; <sup>5</sup>Department of Maternal-Fetal Biology, National Research Institute for Child Health and Development, Tokyo 157-8535, Japan; <sup>6</sup>KOSÉ Corporation, Tokyo 174-0051, Japan; <sup>7</sup>Department of Molecular Biology, Keio University School of Medicine, Tokyo 160-8582, Japan; <sup>8</sup>Division of Diagnostic Pathology, Keio University Hospital, Tokyo 160-8582, Japan; <sup>9</sup>Department of Dermatology, Kyoto University Graduate School of Medicine, Kyoto 606-8507, Japan; <sup>10</sup>Department of Dermatology, Tokyo Medical University, Tokyo 160-0023, Japan; <sup>11</sup>Department of Dermatology, Hamamatsu University School of Medicine, Hamamatsu 431-3192, Japan; <sup>12</sup>Department of Pediatrics, Kyoto University Graduate School of Medicine, Kyoto 606-8507, Japan; <sup>13</sup>Department of Laboratory Medicine, National Center for Child Health and Development, Tokyo 157-8535, Japan; <sup>14</sup>Department of Clinical Genetics, National Center for Child Health and Development, Tokyo 157-8535, Japan; <sup>15</sup>Center for Medical Genetics, Keio University School of Medicine, Tokyo 160-8582, Japan; <sup>16</sup>Laboratory of Gene Medicine, Keio University School of Medicine, Tokyo 160-8582, Japan; <sup>17</sup>Department of Reproductive Biology, National Research Institute for Child Health and Development, Tokyo 157-8535, Japan; <sup>18</sup>Department of Dermatology, School of Medicine, Toho University, Tokyo 143-8540, Japan; <sup>19</sup>Department of Dermatology, National Center for Child Health and Development, Tokyo 157-8535, Japan

\*Correspondence: akiharua@a5.keio.jp

<http://dx.doi.org/10.1016/j.ajhg.2013.09.015>. ©2013 by The American Society of Human Genetics. All rights reserved.



diffuse PPKs show more severe and more progressive features than does NPPK, such as thick hyperkeratosis, leading to flexion contractures (MDM) and constricting bands surrounding the digits (MDM, PPK Gamborg Nielsen, and acral keratoderma), occasionally resulting in spontaneous amputation (MDM and acral keratoderma).<sup>1</sup> NPPK shows only mild and nonprogressive hyperkeratosis and does not show flexion contractures or constricting bands. Thus, NPPK is distinguishable clinically from these other PPKs. Mutations in the coding region of the *SLURP1* (MIM 606119) have been identified in MDM but not in NPPK, suggesting that MDM and NPPK are genetically distinct diseases.<sup>3,12</sup>

To identify gene mutations responsible for NPPK, we performed whole-exome sequencing in three unrelated Japanese NPPK individuals (KDex8 [II-1 of family 1 in Figure 1A], KDex14 [II-2 of family 2], and KDex20 [II-3 of family 3]) who showed the characteristic symptoms of NPPK; Figures 1B and 1C; see Figure S1 available online. Clinical features are summarized in Table 1. The major clinical differentiating points by which we diagnosed these individuals with NPPK among the diverse hereditary PPKs without associated features are summarized in Table 2. The study was conducted after obtaining written informed consent according to the guidelines of the Institutional Review Board of Keio University School of Medicine, National Center for Child Health and Development, Kyoto University, and Tokyo Medical University in accordance with the Helsinki guidelines.

Whole-exome sequencing and data analyses were performed as described previously.<sup>13</sup> Whole-exome sequencing produced approximately 100,000,000 paired reads per sample, approximately 80% of which were mapped to the hs37d5 exon region of the human genome sequence assembly.<sup>14</sup> The average coverage of the exonic region was 87.5×, with more than 93.2% of targeted bases covered at 10× reads. No *SLURP1* mutation (RefSeq: NM\_020427.2) was identified in any of the three NPPK individuals. A genome informatics study found 693, 677, and 747 allelic variants in three NPPK individuals (KDex8, 14, and 20, respectively), showing a minor allele frequency of less than 1% in the 1092 individuals from the 1000 Genomes Project.<sup>14</sup> Because NPPK is possibly inherited in an autosomal recessive manner,<sup>2,3</sup> the causative mutation was expected to be a homozygous or compound heterozygous variant shared by the affected individuals but absent or found only in a heterozygous manner in the control cohort. Among the identified variants, only mutations in the *SERPINB7* (MIM 603357) fulfilled these requirements, suggesting a causative role in NPPK (Table 1).

*SERPINB7* consists of eight exons, with three distinct transcription start sites (exons 1a–c; Figure 2A). The start codon is located within exon 2, and the termination codon within exon 8 (Figure 2A). The *SERPINB7* transcript (RefSeq: NM\_001040147.2) encodes a 380 amino-acid protein. Mutations identified by whole-exome sequencing were confirmed by Sanger sequencing by using the primers

in Table S1 (Figure 2B). A nonsense mutation encoding a c.796C>T alteration (p.Arg266\*) in the last exon of the *SERPINB7* was found in all three NPPK individuals. KDex20 was homozygous for the c.796C>T nonsense mutation. KDex8 was a compound heterozygote of a maternal c.796C>T mutation and a paternal small indel mutation of c.218\_219delAGinsTAAACTTTACCT (c.218\_219del2ins12) at the end of exon 3, predicted to lead to a premature stop codon (p.Gln73Leufs\*17). KDex14 was a compound heterozygote of a maternal c.796C>T mutation and a paternal mutation of c.455-1G>A in the splice acceptor site upstream of exon 6 of *SERPINB7*, which was also predicted to lead to a premature stop codon (p.Gly152Valfs\*21) at chromosome 18: 61465837 in the hs37d5 human genome sequence.<sup>14</sup>

To confirm mutations in *SERPINB7* as a cause of NPPK, we analyzed ten additional unrelated NPPK individuals. The clinical manifestations of these individuals are presented in Table 1. Sanger sequencing failed to detect a mutation in *SLURP1* in any of the ten individuals by using methods described previously.<sup>3</sup> When the entire coding region of *SERPINB7* was analyzed by Sanger sequencing with the primers in Table S1, five of the ten individuals were homozygous for the c.796C>T mutation, four were compound heterozygotes of the c.796C>T and c.218\_219del2ins12 mutations, and one was a compound heterozygote of the c.796C>T and c.455-1G>A mutations (Table 1). These results confirmed that mutations in *SERPINB7* are a major cause of NPPK and that c.796C>T and c.218\_219del2ins12 are major mutations for NPPK in a Japanese population.

From our clinical experience, NPPK is much more common than other types of hereditary PPKs in Japan, although no statistical analysis has been reported. NPPK has not been recognized as a clinical entity within PPKs in Western populations, probably because it is rare. Next, we evaluated the variant databases of the cohort of 1,092 individuals in the 1000 Genomes Project<sup>14</sup> to estimate the frequency of *SERPINB7* mutations classified by ethnicity. The nonsense mutation of c.796C>T was identified as an SNP (rs142859678) with a minor allele frequency of 0.4% and found in a heterozygous manner in two of 89 Japanese individuals, four of 97 Han Chinese individuals from Beijing, and two of 100 Han Chinese individuals from southern China. On the other hand, the c.796C>T mutation was not found in any of 806 non-Asian individuals, suggesting that the c.796C>T mutation is a founder mutation causing NPPK in Asian populations. We also found another putative causative mutation, c.336+2T>G (an SNP of rs201433665), in one of 97 Han Chinese individuals from Beijing in a heterozygous manner. Other mutations found in this study were not identified in the 1,092 individuals.

From these results, the prevalence rate of NPPK was estimated as 1.2/10,000 in Japanese populations and 3.1/10,000 in Chinese populations. In contrast, no putative causative mutation (nonsense, missense, insertion,

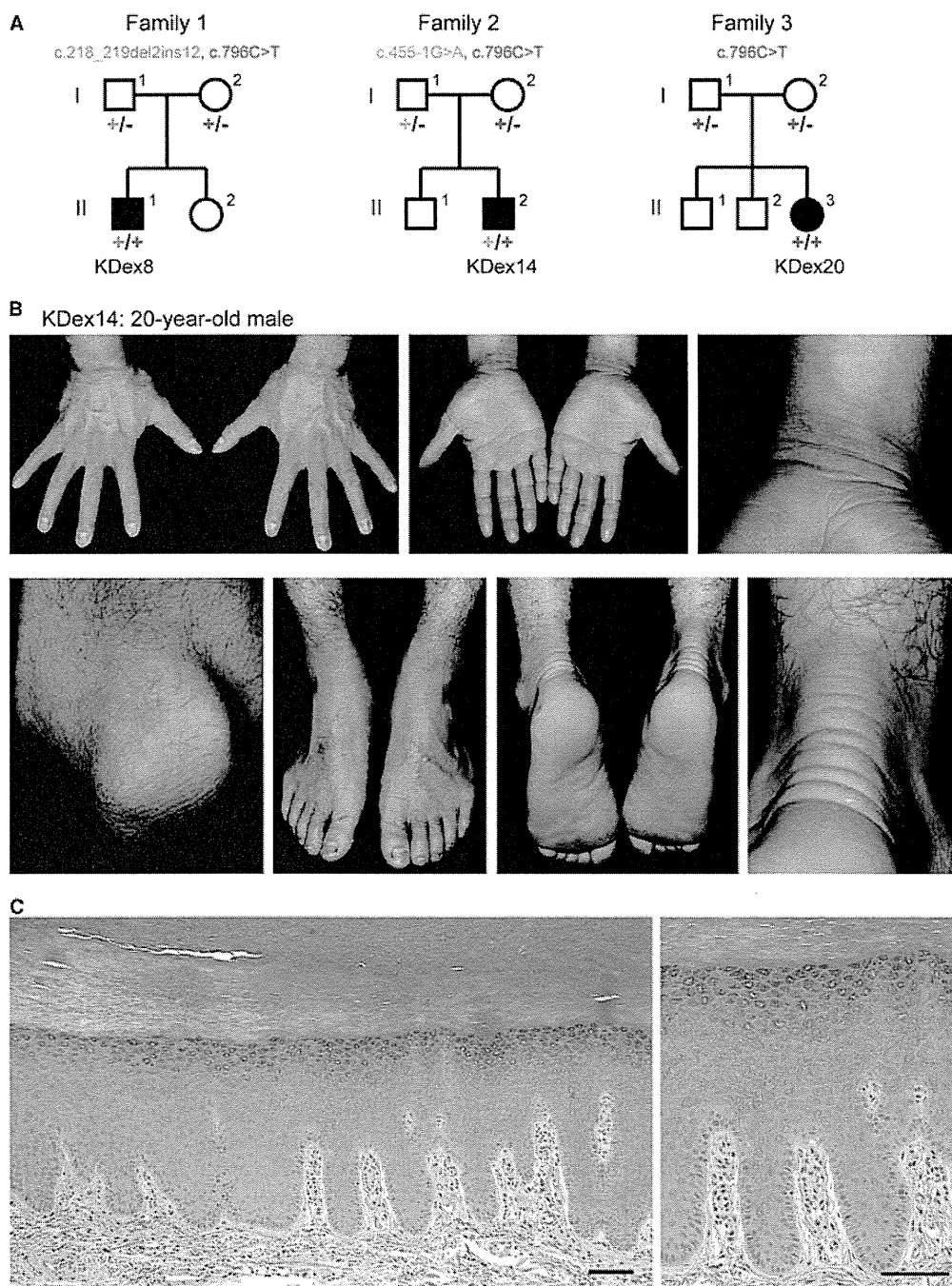


**Figure 1. Family Pedigrees and Skin Manifestations of the Probands with NPPK**

(A) Pedigrees for the families in which exome sequencing and analyses were performed on the probands (KDex8, KDex14, and KDex20). Segregation of the mutations identified in each pedigree is shown.

(B) Skin manifestations of the proband KDex14.

(C) Hematoxylin and eosin staining of the plantar epidermis of the proband KDex8. Scale bars represent 100  $\mu$ m.

deletion, or exon-intron boundary mutation) was identified in 806 individuals of non-Asian origin in the 1000 Genomes Project.<sup>14</sup> We further searched causative mutations in European-American and African-American popu-

lations by using the NHBLI Exome Variant Server and found only one putative causative mutation, c.309delT in the exon 4 (1 of 12,517 alleles), predicted to lead to a premature stop codon (p.Phe103Leufs\*33). Thus, the

**Table 1. SERPINB7 Mutations and Clinical Phenotypes in Individuals with NPPK**

Affected Individual	Gender / Age	Allele 1			Allele 2			Onset	Other Involved Areas	Hyperhidrosis
		Base Change	Amino Acid Change	Segregation	Base Change	Amino Acid Change	Segregation			
<b>Homozygous Mutations</b>										
KDex20 <sup>a</sup>	F/10	c.796C>T	p.Arg266*	Paternal	c.796C>T	p.Arg266*	Maternal	At birth	Knees	+
KDex55	F/2	c.796C>T	p.Arg266*	Paternal	c.796C>T	p.Arg266*	Maternal	Early infancy	–	–
KDex62	M/31	c.796C>T	p.Arg266*	NA	c.796C>T	p.Arg266*	NA	1 week	Knees	+
KDex72	F/5	c.796C>T	p.Arg266*	Paternal	c.796C>T	p.Arg266*	Maternal	At birth	Knees and elbows	+
KDex79	M/31	c.796C>T	p.Arg266*	NA	c.796C>T	p.Arg266*	NA	At birth	Knees and elbows	+
KDex90	M/14	c.796C>T	p.Arg266*	Paternal	c.796C>T	p.Arg266*	Maternal	9-10 years	Knees and elbows	+
<b>Compound Heterozygous Mutations</b>										
KDex8 <sup>a</sup>	M/38	c.796C>T	p.Arg266*	Maternal	c.218_219del2ins12	p.Gln73Leufs*17 <sup>b</sup>	Paternal	At birth	Knees and elbows	+
KDex59	F/16	c.796C>T	p.Arg266*	Paternal	c.218_219del2ins12	p.Gln73Leufs*17 <sup>b</sup>	Maternal	At birth	–	+
KDex60	F/30	c.796C>T	p.Arg266*	Paternal	c.218_219del2ins12	p.Gln73Leufs*17 <sup>b</sup>	Maternal	At birth	Knees	+
KDex64	F/28	c.796C>T	p.Arg266*	Paternal	c.218_219del2ins12	p.Gln73Leufs*17 <sup>b</sup>	Maternal	2 years	–	+
KDex66	F/64	c.796C>T	p.Arg266*	NA	c.218_219del2ins12	p.Gln73Leufs*17 <sup>b</sup>	NA	Early infancy	–	–
KDex14 <sup>a</sup>	M/20	c.796C>T	p.Arg266*	Maternal	c.455-1G>A	p.Gly152Valfs*21 <sup>b</sup>	Paternal	At birth	Knees and elbows	+
KDex58	M/51	c.796C>T	p.Arg266*	NA	c.455-1G>A	p.Gly152Valfs*21 <sup>b</sup>	NA	5–6 years	Knees and elbows	+

Abbreviations: M, male; F, Female; NA, not available; c.218\_219del2ins12, c.218\_219delAGinsTAAACTTTACCT.

<sup>a</sup>Whole-exome sequencing performed.<sup>b</sup>Predicted from genomic sequences.

**Table 2. Major Clinical Differentiating Points among Diffuse Hereditary Palmoplantar Keratoses without Associated Features**

Types	Vörner <sup>37</sup>	Unna-Thost <sup>38,39</sup>	Greither <sup>40</sup>	Sybert <sup>41</sup>	Bothnian <sup>31</sup>	Mal de Meleda <sup>8</sup>	Nagashima <sup>2,3</sup>	Gamborg Nielsen <sup>9,10</sup>	Acral Keratoderma <sup>11</sup>
Other names	Diffuse Epidermolytic PPK	Diffuse Nonepidermolytic PPK	Progressive PPK			Keratosis Palmoplantaris Transgradiens of Siemens			
MIM number	144200	600962	144200		600231	248300		244850	
Mode of inheritance	AD	AD	AD	AD	AD	AR	AR	AR	AR
Responsible gene	<i>KRT1</i> <sup>42</sup> <i>KRT9</i> <sup>43,44</sup>	<i>KRT1</i> <sup>45</sup>	<i>KRT1</i> <sup>46</sup>	Unknown	<i>AQPS</i> <sup>42,43</sup>	<i>SLURP1</i> <sup>12</sup>	<i>SERPINB7</i> <sup>3</sup>	Unknown	Unknown
Prevalence rate	4.4/100,000 populations in Northern Ireland <sup>47</sup>	Clinical entity in doubt <sup>1,48,49</sup>	Rare	Rare	Rare	Relatively common in the island of Meleda. 1/100,000 in general populations <sup>50</sup>	1.2/10,000 in Japan <sup>a</sup> , 3.1/10,000 in China <sup>b</sup>	Rare	Rare
Age of onset	Within the first year of life	Within the first 2 years of life	Ages 8 to 10	Within the first year of life	During childhood, not as early as during the first year of life	Early infancy	Mostly within the first year of life		
Pathologic findings	Epidermolytic hyperkeratosis	Nonepidermolytic	Nonepidermolytic	Nonepidermolytic	Nonepidermolytic	Nonepidermolytic	Nonepidermolytic	Nonepidermolytic	Nonepidermolytic
Hyperkeratosis	Thick	Thick	Thick	Thick	Mild to thick	Severe	Mild	Thick	Thick
Transgradiens	–	–	+	+	+	+	+	+ (1 of 4)	+
Hyperhidrosis	–	–	+	Not described	+	+	+	Not described	Not described
Whitish change upon water exposure	–	–	–	–	+	–	+	–	–
Development on other areas	–	–	Elbows, knees, flexural areas, and Achilles tendon	Natal cleft, groin, elbows, knees, posterior aspects of forearms, and anterior aspects of legs	–	Knees and elbows, perioral erythema, and periorbital erythema	Knees, elbows, and Achilles tendon area	Only knuckle pads on the dorsa of the fingers	Knees, elbows, ankles, Achilles tendon area
Constricting bands	–	–	+	+	–	+	–	+	+
Spontaneous amputation	–	–	+	+	–	Occasionally	–	Not described	+
Flexion contractures	–	–	–	–	–	+	–	–	–

Abbreviations: AD, autosomal dominant inheritance; AR, autosomal recessive inheritance.  
<sup>a</sup>This study.



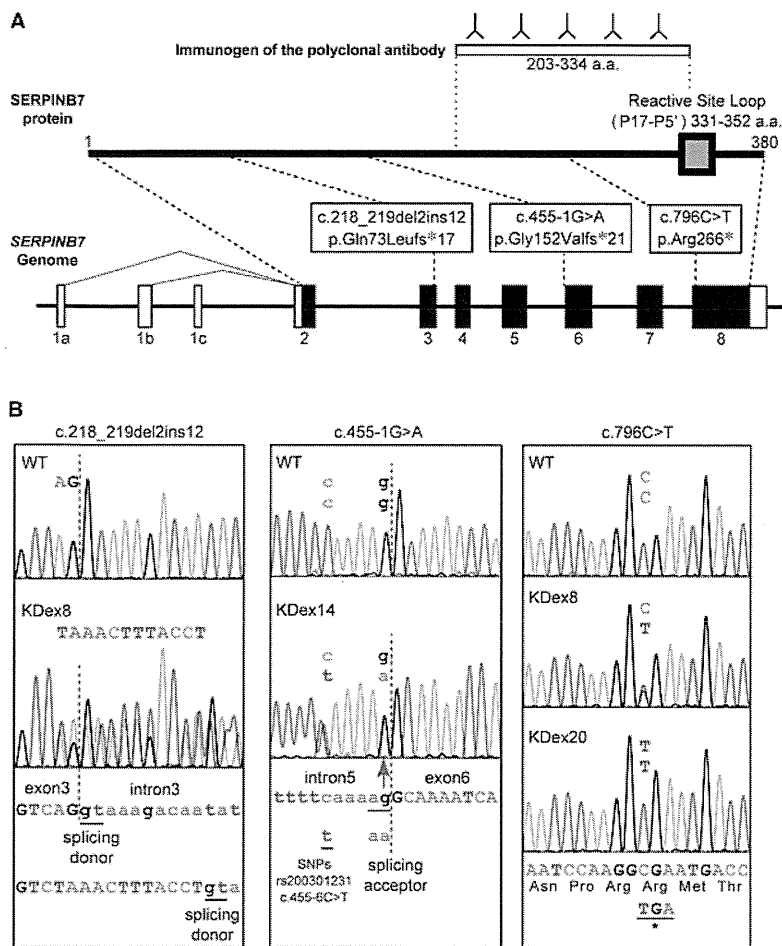


**Figure 2. Genomic Organization of *SERPINB7*, Reactive Site Loop for Protease Inhibitory Activity of the *SERPINB7* Protein, and Location of NPPK-Causing Mutations**

(A) Schematic presentation of the genomic structure of *SERPINB7* (lower) and its encoded protein (middle), *SERPINB7*. The gray box indicates the reactive site loop indispensable for protease inhibitory activity of *SERPINB7*. Open and filled boxes indicate exons of untranslated regions and coding regions, respectively. The positions of *SERPINB7* mutations identified in this study are indicated. The immunogen of the anti-*SERPINB7* polyclonal antibody is shown at the top.

(B) Heterozygous or homozygous mutated sequences of affected individuals (KDex8, KDex14, and KDex20) compared with the corresponding wild-type sequences. The base and amino acid sequences are shown. The intron-exon junctions are shown with red dotted lines. Intron and exon sequences are shown in lower case and upper case, respectively.

Abbreviations are as follows: c.218\_219del2ins12, c.218\_219delAGinsTAAACTTTACCT.

*SERPINB7* is located on chromosome 18q21.3, forming a cluster of clade-B serpin genes.<sup>18</sup> Clade-B serpins are intracellular serpins, possibly protecting cells from exogenous and endogenous protease-mediated injury.<sup>18</sup> The protease-inhibitory activity of serpins is dependent on the reactive site loop to form a covalent

prevalence rate of NPPK in non-Asian populations was ~0.5/100,000,000. These results well explain why NPPK is so common in PPKs in Japanese populations but has not been reported from non-Asian countries.

Serpins were originally identified as serine protease inhibitors. Serpin molecules are evolutionarily old because even bacteria and Archaea possess them.<sup>15–17</sup> Most serpins identified to date possess protease inhibitory activity, although their protease targets are now known not to be restricted to serine proteases.<sup>16,17</sup> Serpins form covalent complexes with target proteases to inhibit protease activity irreversibly. Human serpins have been divided into nine clades (A–I) by phylogenetic analyses.<sup>15,18</sup> Several congenital diseases have been reported to be caused by deficiencies in the protease inhibitory function of serpins—for example, plasminogen activator inhibitor-1 deficiency (MIM 613329) with mutations in *SERPINE1* (MIM 173360)<sup>19</sup>—or to be caused by polymerization and accumulation of mutated serpins, for example, familial encephalopathy with neuroserpin inclusion bodies (MIM 604218) with mutations in *SERPINI1* (MIM 602445).<sup>20</sup>

bond with target proteases.<sup>16</sup> The center of the reactive site loop (P1–P1′) is located at amino acids 347–348 of *SERPINB7*,<sup>16</sup> and the entire region of the reactive site loop (P17–P5′, corresponding to the amino acid region 331–352 of *SERPINB7*) is predicted to be absent in all of the mutant proteins (Figure 2A). Thus, all of the mutations identified in this study presumably result in a complete loss of the protease inhibitory activity of *SERPINB7*.

*SERPINB7* was originally described as being expressed in kidney mesangial cells and was named *MEGSIN*.<sup>21</sup> However, no renal manifestation has been identified in NPPK individuals. A recent report using a bacterial artificial chromosome transgene expressing Cre in mice under the control of *Serp7* regulatory elements showed specific expression of Cre in cornified stratified epithelial cells, but not in kidney mesangial cells,<sup>22</sup> suggesting that *Serp7* might be specifically expressed in epidermal keratinocytes in mice. Thus, we next analyzed the expression of *SERPINB7* in human skin. We used a commercial polyclonal antibody (HPA024200; Sigma-Aldrich) raised against a peptide corresponding to the amino acid 203–334 region of human *SERPINB7* (Figure 2A). To characterize

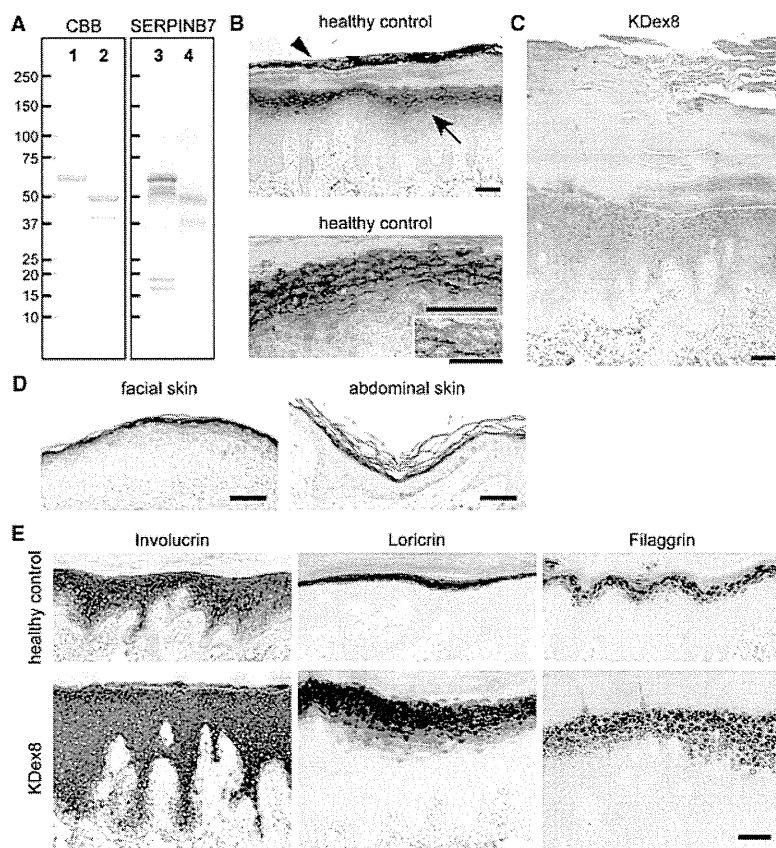


**Figure 3. SERPINB7 Localization in the Epidermis and Immunohistochemical Analysis of the Affected Skin**

(A) Investigation of the anti-SERPINB7 antibody. GST-fused recombinant full-length human SERPINB7 (lanes 1 and 3) and GST-fused recombinant p.Arg266\* mutant (lanes 2 and 4) were analyzed by electrophoresis with Coomassie Brilliant Blue staining (lanes 1 and 2) or with immunoblotting with the anti-SERPINB7 rabbit polyclonal antibody (lanes 3 and 4). Scale bars indicate molecular weights (kDa). (B) Immunohistochemistry of SERPINB7 in plantar skin of a healthy control. Upper panel shows SERPINB7 in the stratum granulosum (arrow) and in the upper part of the stratum corneum (arrowhead). Lower panel shows the intracellular distribution of SERPINB7 in the stratum granulosum. Scale bars represent 100  $\mu$ m. Inset in the lower panel shows stratum granulosum cells and intercellular spaces at higher magnification (scale bar represents 50  $\mu$ m). (C) Immunohistochemistry of SERPINB7 in the hyperkeratotic plantar skin of NPPK individual of KDex8. Scale bar represents 100  $\mu$ m. (D) Immunohistochemistry of SERPINB7 in facial and abdominal skin sections of a healthy control. Scale bars represent 100  $\mu$ m. (E) Immunohistochemistry of epidermal differentiation-related proteins in plantar skin of a healthy control (upper panels) and a NPPK individual (KDex8; lower panels). Scale bar represents 100  $\mu$ m.

the antibody, we performed immunoblotting against GST-fused full-length human SERPINB7 and GST-fused p.Arg266\* mutant that were produced in *Escherichia coli* BL21(DE3) by using the pGEX 5X-1 vector (GE Healthcare) in inclusion bodies and purified by washing with 1% Triton X-100 and 4 M urea. The purified proteins showed molecular weights of ~62 kDa and ~50 kDa in SDS-PAGE analysis, respectively (Figure 3A). In immunoblotting analysis, the anti-SERPINB7 antibody recognized both the GST-fused full-length SERPINB7 and GST-fused p.Arg266\* mutant (Figure 3A). The immunosignals for the full-length SERPINB7 were stronger than those for the truncated p.Arg266\* mutant, suggesting that this polyclonal antibody includes antibodies against peptides corresponding to both the amino acid 203–265 region and the 266–334 region of human SERPINB7 (Figure 2A).

Using this antibody, we performed an immunohistochemical analysis of paraffin wax-embedded sections of healthy human skin and NPPK skin, with antigen retrieval with 15 min boiling in a microwave oven in 100 mM Tris-HCl and 1 mM EDTA buffer (pH 9.0), immunosignal detection with ImmPRESS kit and NovaRed substrates (Vector Laboratories), and counterstaining with methyl green (Wako Pure Chemical). The immunosignals of the antibody were specifically detected from the stratum granulosum and from the upper part of the SC in healthy control

plantar skin (Figure 3B). No signal was detected from the lower part of the SC, probably because the tightly packed intracorneocyte proteinaceous structure prevents access of the antibody to the antigen. When the stratum granulosum was observed at higher magnification, signals were observed in the cytoplasm, with a mild concentration to the apical side of the stratum granulosum cells (Figure 3B). In NPPK individuals, the immunosignals of the stratum granulosum and the SC were markedly diminished (KDex8, a compound heterozygote of the c.796C>T and c.218\_219del2ins12 mutations; Figure 3C. For other affected individuals, data are not shown or skin biopsies were not performed). Thus, the immunosignals observed in healthy control plantar skin were considered to represent the distribution of SERPINB7. Some nuclear staining was observed in both the healthy control skin and the NPPK skin, which was considered to be nonspecific background (Figures 3B and 3C). Weak cytoplasmic immunosignals were observed in the NPPK skin, which were considered to be due to the p.Arg266\* mutant of SERPINB7 or nonspecific background (Figure 3C).

To clarify whether *SERPINB7* expression was limited to the palmoplantar area of the skin, we immunostained facial and abdominal skin sections of healthy controls. SERPINB7 immunosignals were specifically detected from the stratum granulosum and the SC in facial and abdominal epidermis

(Figure 3D), suggesting that *SERPINB7* is expressed in the epidermis of the whole body.

Next, we investigated whether loss of functional *SERPINB7* affected epidermal differentiation by using NPPK skin. In NPPK plantar skin, hematoxylin and eosin staining showed acanthosis and orthohyperkeratosis (Figure 1C), as described previously.<sup>3</sup> The localization of epidermal differentiation markers, loricrin, involucrin, and filaggrin, which were detected with anti-loricrin (ab24722; Abcam), anti-involucrin (clone SY5; Sigma Aldrich), and anti-filaggrin (clone FLG01; Thermo Scientific) antibodies, respectively, showed no major keratinocyte differentiation defect in NPPK skin (Figure 3E). Transmission electron microscopic studies of NPPK skin failed to show any major defect in the stratum granulosum or the SC (data not shown).

Loss of functional *SERPINB7* might induce overactivation of target proteases in the stratum granulosum and the SC. Because no apparent change was observed in the stratum granulosum except for thickening, we reinvestigated the skin phenotype of NPPK, looking especially for any finding of changes in the SC. We found that the NPPK skin showed a whitish spongy appearance within 10 min of water exposure specifically in the reddish hyperkeratotic area (Figure 4A). The wrinkling of palms that is observed after water exposure in cystic fibrosis (MIM 219700)<sup>23,24</sup> was not apparent, even after 30 min of water exposure (Figure 4A). These phenotypes suggested enhanced water permeation into the surface of the SC in NPPK lesional skin.

Thus, we next performed a transepidermal water loss (TEWL) analysis prior to and after water exposure in three NPPK individuals and three healthy controls. TEWL was measured at the lesional and nonlesional skin of dorsal hands and inner wrists in each NPPK individual and at the corresponding skin area in each healthy control with a Vapo Scan AS-VT100RS (Asahi Biomed) at room temperature (20°C–22°C) and 40%–60% humidity to avoid the effects of hyperhidrosis. The mean TEWL value was calculated from measurements of at least eight different points under each skin condition. Before water exposure, the mean TEWL values were higher in the lesional skin of NPPK individuals than in the nonlesional skin of NPPK individuals or the corresponding skin area of normal healthy controls (Figure 4B), when analyzed by using the Tukey-Kramer multiple-comparisons test with the Prism software (ver. 6; GraphPad Software). Next, the hands of NPPK individuals and healthy controls were immersed in water at 37°C for 30 min. After water exposure, TEWL values were significantly elevated in all skin conditions in all NPPK skin and in all healthy control skin (data not shown), and the mean TEWL values were significantly elevated on water exposure in any skin condition (Figure 4B) when analyzed with Student's *t* test with the Prism software.

After water exposure, the mean TEWL values were higher in the lesional skin of NPPK individuals than in

the nonlesional skin of NPPK individuals or the corresponding skin areas of healthy controls (Figure 4B) when analyzed with the Tukey-Kramer multiple-comparisons test. Because the TEWL instrument measures water evaporation from the skin surface, the TEWL values after water exposure might correspond mostly to water evaporation from water-swollen SC. Thus, these results suggest that water permeation into the SC is specifically facilitated in NPPK lesional skin.

Here, we identified that loss-of-function mutations in *SERPINB7* cause NPPK and established NPPK genetically as a distinct clinical entity within hereditary diffuse PPKs without associated features. While *SERPINB7* was considered to be expressed in the epidermis of the whole body, the affected skin area of NPPK is limited to hands, feet, knees, and elbows, the reason for which remains unknown. Such limitations in the affected skin area with a deficiency of gene products that are ubiquitously expressed in the epidermis have been observed in several other types of PPK: Vohwinkel syndrome (MIM 124500), caused by mutations in *GJB2* (MIM 121011),<sup>25</sup> and type I striate PPK (MIM 148700), caused by mutations in *DSG1* (MIM 125670).<sup>26</sup> The effects on the knees and elbows in NPPK suggest that chronic exposure to mechanical stress might have a role in the development of NPPK skin lesions, and the lesions in NPPK are limited to chronic mechanical stress-exposed areas of the skin. Thus, *SERPINB7* might inhibit mechanical stress-induced proteases and protect keratinocytes or corneocytes from protease-mediated cellular damage.

Our findings suggest that NPPK is a genetic dermatosis caused by a deficiency of an intracellular protease inhibitor. Deficiencies of the protease inhibitors, LEKTI, encoded by *SPINK5* (MIM 605010), and cystatin A, encoded by *CSTA* (MIM 184600), have been reported in Netherton syndrome (MIM 256500)<sup>27</sup> and exfoliative ichthyosis (MIM 607936),<sup>28</sup> respectively. In Netherton syndrome, overactivation of secreted extracellular proteases, kallikreins, has been suggested to induce overdesquamation via excessive degradation of cell adhesion molecules in the SC<sup>29</sup> and skin inflammatory responses through thymic stromal lymphopoietin expression, mediated by unregulated activation of protease-activated receptor-2.<sup>30</sup> In exfoliative ichthyosis, defects in desmosome-mediated cell-cell adhesion in the lower levels of the epidermis have been suggested to cause coarse peeling of skin on the palms and soles.<sup>28</sup> However, the precise pathophysiology or protease overactivation induced by the loss of cystatin A has not yet been characterized.

As corneocytes lose the cell membrane on cornification, it is unclear whether *SERPINB7* is held within corneocytes at the SC. But the phenotype of NPPK differs completely from that of Netherton syndrome because desquamation is rather prolonged in the erythematous hyperkeratotic area in NPPK, suggesting that the target proteases of *SERPINB7* are unlikely to be associated with the desquamation process. Here, we observed a whitish spongy change

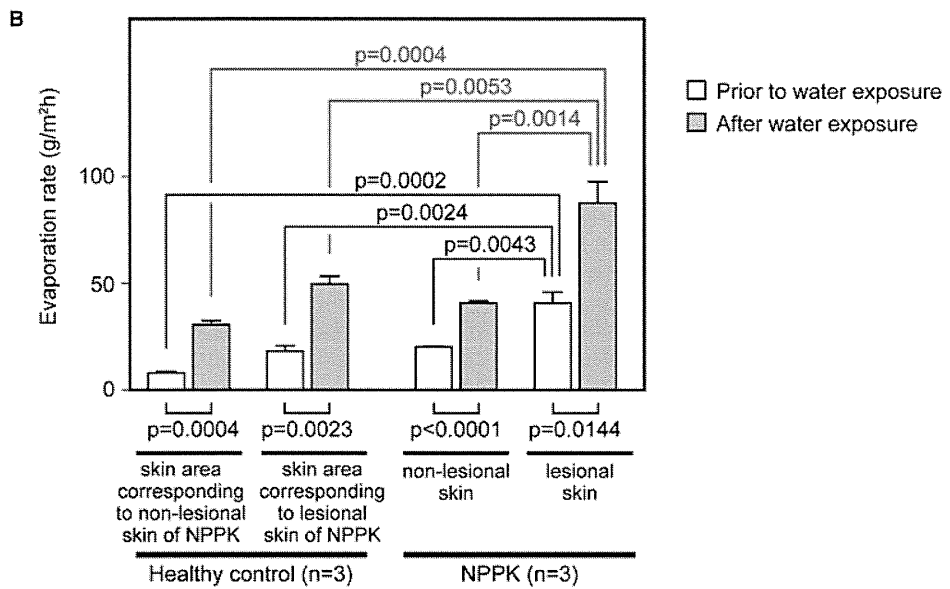
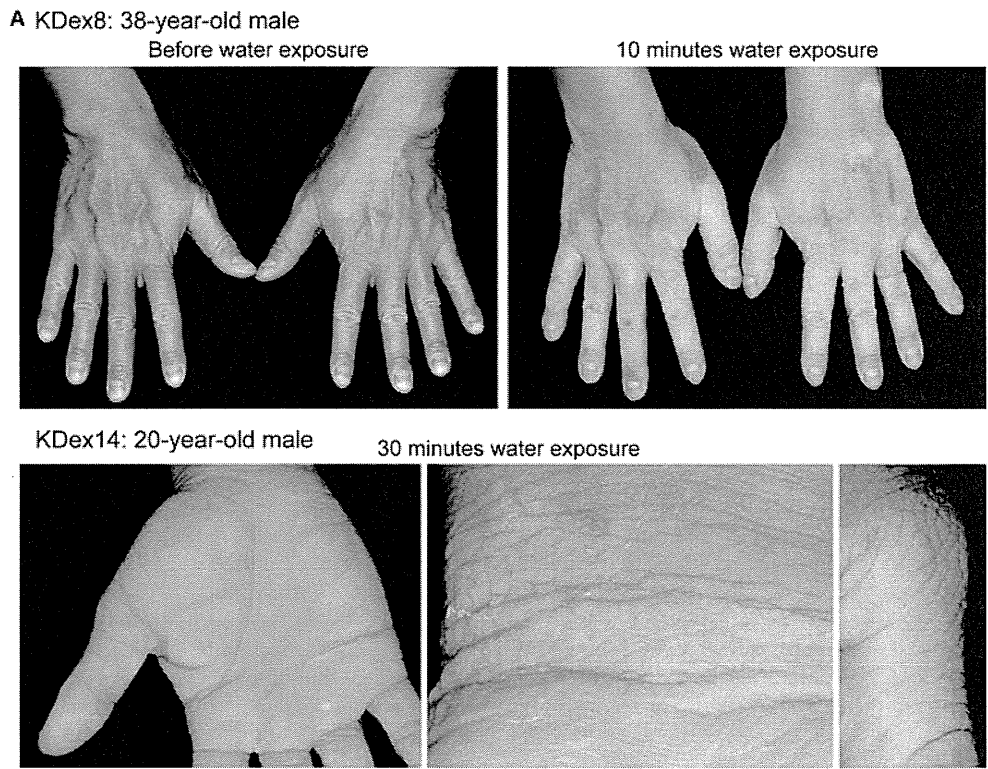


**Figure 4. Changes upon Water Exposure in NPPK Lesional Skin**

(A) Clinical phenotype of the hands of the proband (KDex8) prior to water exposure (upper left panel) and after 10 min water exposure (upper right panel), and the clinical phenotype of the hands of the proband (KDex14) after 30 min water exposure: the palm (lower left panel), inner wrist (lower middle panel), and dorsal of the thumb (lower right panel).

(B) Means of TEWL values prior to water exposure and after 30 min of water exposure in the lesional skin and nonlesional skin of NPPK individuals (n = 3; KDex8, KDex14, and KDex79) and in the corresponding skin area of healthy controls (n = 3). In each skin condition, the means of TEWL were compared upon water exposure (lower lines). The means of TEWL were compared between lesional and nonlesional skin of NPPK individuals and the corresponding skin area of healthy controls before water exposure (upper black lines) and after water exposure (upper red lines).

in the SC on exposure to water in the lesional skin of NPPK. This change is caused by a loss of integrity in the SC structure, probably due to overactivation of target proteases of SERPINB7. Such a whitish change in the skin upon water exposure has been reported in an autosomal-dominant Bothnian-type PPK (MIM 600231) with mutations in *AQP5* (MIM 600442),<sup>31–33</sup> and in the aquagenic keratoderma associated with cystic fibrosis with mutations in *CFTR* (MIM 602421),<sup>23,24</sup> but the pathophysiology of the whitish changes might differ among these diseases.

Together with the strong immunosignals of SERPINB7 in the SC, we propose that loss of functional SERPINB7 induces overactivation of intracorneocyte proteases specifically in the affected skin area, which induces degradation of the integrated proteinaceous structure of the corneocytes and facilitates water permeation into the SC. Additional functional assays and molecular biological analyses are required to investigate the changes in the water repellent properties of the SC surface in NPPK skin.

Various proteases are present in the stratum granulosum and the SC<sup>34–36</sup>. Additionally, the epidermis is attacked by various exogenous proteases—originating from bacteria, fungi, virus, pollen, and house dust mites—and endogenous proteases, originating from infiltrating cells.<sup>35</sup> Appropriate control of the activity of these proteases by endogenous protease inhibitors is likely important in maintaining skin homeostasis. Our discovery of loss-of-function mutations in *SERPINB7* in NPPK should provide insights into the functions and regulatory mechanisms of proteases and protease inhibitors in the epidermis. Future studies will aim to identify the target proteases of SERPINB7 in the steady state and in mechanically stressed states. It is also important to understand the pathophysiology of the putative protease overactivation in NPPK skin; that is, how the proteinaceous structure of the SC and integrity of the SC barrier are affected and whether the reddish hyperkeratosis and inflammatory cell infiltrations are secondary changes via augmented external stimuli through protease-mediated damage to the SC or direct effects of intraepidermal overactivation of proteases. The development of specific protease inhibitors mimicking SERPINB7 might allow pathogenesis-based therapies for NPPK.

#### Supplemental Data

Supplemental Data includes one figure and one table and can be found with this article online at <http://www.cell.com/AJHG/home>.

#### Acknowledgments

We thank our clinical colleagues, and family members who contributed the samples used in this study. We also thank Nobuyo Nishimura, Hiromi Sakuragi, Asami Hirakiyama, Kazunari Shibata, and the Collaborative Research Resources of Keio University School of Medicine for technical support. This work was supported in parts by Health and Labour Sciences Research Grants for Research on Rare and Intractable Diseases, for Research on Allergic

Disease and Immunology, and for Research on Measures for Intractable Diseases from the Ministry of Health, Labour and Welfare of Japan, The Grant of National Center for Child Health and Development (24-5), and Grants-in-Aid for Scientific Research from the Ministry of Education, Culture, Sports, Science and Technology, Japan. This manuscript is dedicated to the memory of Professor Masaji Nagashima. Potential conflict of interest: M.A. has consultancy arrangements with Daiichi Sankyo Co. A.K., A.S., and T.S. have been supported by one or more grants from MSD K.K. and Maruho Co., Ltd. This work was supported in part by a grant from Maruho Co., Ltd.

Received: August 23, 2013

Revised: September 19, 2013

Accepted: September 25, 2013

Published: October 24, 2013

#### Web Resources

The URLs for data presented here are as follows:

1000 Genomes, <http://browser.1000genomes.org>  
NCBI dbSNPs, <http://www.ncbi.nlm.nih.gov/projects/SNP/>  
NCBI RefSeq, <http://www.ncbi.nlm.nih.gov/refseq/>  
NHLBI Exome Sequencing Project (ESP) Exome Variant Server, <http://evs.gs.washington.edu/EVS/>  
Online Mendelian Inheritance in Man (OMIM), <http://www.omim.org/>

#### References

1. Lucker, G.P., Van de Kerkhof, P.C., and Steijlen, P.M. (1994). The hereditary palmoplantar keratoses: an updated review and classification. *Br. J. Dermatol.* *131*, 1–14.
2. Mitsuhashi, Y., and Hashimoto, I. (1989). Keratosis palmoplantaris Nagashima. *Dermatologica* *179*, 231.
3. Kabashima, K., Sakabe, J., Yamada, Y., and Tokura, Y. (2008). “Nagashima-type” keratosis as a novel entity in the palmoplantar keratoderma category. *Arch. Dermatol.* *144*, 375–379.
4. Mitsuhashi, Y., Hashimoto, I., and Takahashi, M. (1989). Meleda type keratosis palmoplantaris (Nagashima). *Practical Dermatol.* *11*, 297–300, (in Japanese).
5. Nagashima, M. (1977). Palmoplantar keratoses. In *Handbook of Human Genetics, Volume 9*, O. Miura and K. Ochiai, eds. (Tokyo: Igaku Shoin), pp. 23–27, (in Japanese).
6. Isoda, H., Kabashima, K., and Tokura, Y. (2009). ‘Nagashima-type’ keratosis palmoplantaris in two siblings. *J. Eur. Acad. Dermatol. Venereol.* *23*, 737–738.
7. Sakabe, J., Kabashima, K., Sugita, K., and Tokura, Y. (2009). Possible involvement of T lymphocytes in the pathogenesis of Nagashima-type keratosis palmoplantaris. *Clin. Exp. Dermatol.* *34*, e282–e284.
8. Hovorka, O., and Ehlers, E. (1897). Mal de Meleda. *Arch. Dermatol. Res.* *40*, 251–256.
9. Gamborg Nielsen, P. (1985). Two different clinical and genetic forms of hereditary palmoplantar keratoderma in the northernmost county of Sweden. *Clin. Genet.* *28*, 361–366.
10. Kastl, I., Anton-Lamprecht, I., and Gamborg Nielsen, P. (1990). Hereditary palmoplantar keratosis of the Gamborg Nielsen type. Clinical and ultrastructural characteristics of a new type of autosomal recessive palmoplantar keratosis. *Arch. Dermatol. Res.* *282*, 363–370.

11. Nesbitt, L.T., Jr., Rothschild, H., Ichinose, H., Stein, W., 3rd, and Levy, L. (1975). Acral keratoderma. *Arch. Dermatol.* *111*, 763–768.
12. Fischer, J., Bouadjar, B., Heilig, R., Huber, M., Lefèvre, C., Jobard, F., Macari, F., Bakija-Konsuo, A., Ait-Belkacem, F., Weissenbach, J., et al. (2001). Mutations in the gene encoding SLURP-1 in Mal de Meleda. *Hum. Mol. Genet.* *10*, 875–880.
13. Sasaki, T., Niizeki, H., Shimizu, A., Shiohama, A., Hirakiyama, A., Okuyama, T., Seki, A., Kabashima, K., Otsuka, A., Ishiko, A., et al. (2012). Identification of mutations in the prostaglandin transporter gene *SLCO2A1* and its phenotype-genotype correlation in Japanese patients with pachydermoperiostosis. *J. Dermatol. Sci.* *68*, 36–44.
14. The 1000 Genomes Project Consortium. (2012). An integrated map of genetic variation from 1,092 human genomes. *Nature* *491*, 56–65.
15. Irving, J.A., Pike, R.N., Lesk, A.M., and Whisstock, J.C. (2000). Phylogeny of the serpin superfamily: implications of patterns of amino acid conservation for structure and function. *Genome Res.* *10*, 1845–1864.
16. Gettins, P.G.W. (2002). Serpin structure, mechanism, and function. *Chem. Rev.* *102*, 4751–4804.
17. Law, R.H.P., Zhang, Q., McGowan, S., Buckle, A.M., Silverman, G.A., Wong, W., Rosado, C.J., Langendorf, C.G., Pike, R.N., Bird, P.I., and Whisstock, J.C. (2006). An overview of the serpin superfamily. *Genome Biol.* *7*, 216.
18. Silverman, G.A., Whisstock, J.C., Askew, D.J., Pak, S.C., Luke, C.J., Cataltepe, S., Irving, J.A., and Bird, P.I. (2004). Human clade B serpins (ov-serpins) belong to a cohort of evolutionarily dispersed intracellular proteinase inhibitor clades that protect cells from promiscuous proteolysis. *Cell. Mol. Life Sci.* *61*, 301–325.
19. Fay, W.P., Shapiro, A.D., Shih, J.L., Schleef, R.R., and Ginsburg, D. (1992). Brief report: complete deficiency of plasminogen-activator inhibitor type 1 due to a frame-shift mutation. *N. Engl. J. Med.* *327*, 1729–1733.
20. Davis, R.L., Shrimpton, A.E., Carrell, R.W., Lomas, D.A., Gerhard, L., Baumann, B., Lawrence, D.A., Yepes, M., Kim, T.S., Ghetti, B., et al. (2002). Association between conformational mutations in neuroserpin and onset and severity of dementia. *Lancet* *359*, 2242–2247.
21. Miyata, T., Nangaku, M., Suzuki, D., Inagi, R., Urugami, K., Sakai, H., Okubo, K., and Kurokawa, K. (1998). A mesangium-predominant gene, *megsin*, is a new serpin upregulated in IgA nephropathy. *J. Clin. Invest.* *102*, 828–836.
22. Wang, Y., Guo, Q., Casey, A., Lin, C., and Chen, F. (2012). A new tool for conditional gene manipulation in a subset of keratin-expressing epithelia. *Genesis* *50*, 899–907.
23. Garçon-Michel, N., Roguedas-Contios, A.-M., Rault, G., Le Bihan, J., Ramel, S., Revert, K., Dirou, A., and Misery, L. (2010). Frequency of aquagenic palmoplantar keratoderma in cystic fibrosis: a new sign of cystic fibrosis? *Br. J. Dermatol.* *163*, 162–166.
24. Weibel, L., and Spinaz, R. (2012). Images in clinical medicine. Aquagenic wrinkling of palms in cystic fibrosis. *N. Engl. J. Med.* *366*, e32.
25. Maestrini, E., Korge, B.P., Ocaña-Sierra, J., Calzolari, E., Cambiaggi, S., Scudder, P.M., Hovnanian, A., Monaco, A.P., and Munro, C.S. (1999). A missense mutation in *connexin26*, D66H, causes mutilating keratoderma with sensorineural deafness (Vohwinkel's syndrome) in three unrelated families. *Hum. Mol. Genet.* *8*, 1237–1243.
26. Rickman, L., Simrak, D., Stevens, H.P., Hunt, D.M., King, I.A., Bryant, S.P., Eady, R.A., Leigh, I.M., Arnemann, J., Magee, A.I., et al. (1999). N-terminal deletion in a desmosomal cadherin causes the autosomal dominant skin disease striate palmoplantar keratoderma. *Hum. Mol. Genet.* *8*, 971–976.
27. Chavanas, S., Bodemer, C., Rochat, A., Hamel-Teillac, D., Ali, M., Irvine, A.D., Bonafé, J.L., Wilkinson, J., Taieb, A., Barrandon, Y., et al. (2000). Mutations in *SPINK5*, encoding a serine protease inhibitor, cause Netherton syndrome. *Nat. Genet.* *25*, 141–142.
28. Blaydon, D.C., Nitoiu, D., Eckl, K.-M., Cabral, R.M., Bland, P., Hausser, I., van Heel, D.A., Rajpopat, S., Fischer, J., Oji, V., et al. (2011). Mutations in *CSTA*, encoding Cystatin A, underlie exfoliative ichthyosis and reveal a role for this protease inhibitor in cell-cell adhesion. *Am. J. Hum. Genet.* *89*, 564–571.
29. Descargues, P., Deraison, C., Bonnart, C., Kreft, M., Kishibe, M., Ishida-Yamamoto, A., Elias, P., Barrandon, Y., Zambruno, G., Sonnenberg, A., and Hovnanian, A. (2005). *Spink5*-deficient mice mimic Netherton syndrome through degradation of desmoglein 1 by epidermal protease hyperactivity. *Nat. Genet.* *37*, 56–65.
30. Briot, A., Deraison, C., Lacroix, M., Bonnart, C., Robin, A., Besson, C., Dubus, P., and Hovnanian, A. (2009). Kallikrein 5 induces atopic dermatitis-like lesions through PAR2-mediated thymic stromal lymphopoietin expression in Netherton syndrome. *J. Exp. Med.* *206*, 1135–1147.
31. Lind, L., Lundström, A., Hofer, P.A., and Holmgren, G. (1994). The gene for diffuse palmoplantar keratoderma of the type found in northern Sweden is localized to chromosome 12q11-q13. *Hum. Mol. Genet.* *3*, 1789–1793.
32. Blaydon, D.C., Lind, L.K., Plagnol, V., Linton, K.J., Smith, F.J.D., Wilson, N.J., McLean, W.H.I., Munro, C.S., South, A.P., Leigh, I.M., et al. (2013). Mutations in *AQP5*, Encoding a Water-Channel Protein, Cause Autosomal-Dominant Diffuse Nonepidermolytic Palmoplantar Keratoderma. *Am. J. Hum. Genet.* *93*, 330–335.
33. Cao, X., Yin, J., Wang, H., Zhao, J., Zhang, J., Dai, L., Zhang, J., Jiang, H., Lin, Z., and Yang, Y. (2013). Mutation in *AQP5*, Encoding Aquaporin 5, Causes Palmoplantar Keratoderma Bothnia Type. *J. Invest. Dermatol.*, in press.
34. Kamata, Y., Taniguchi, A., Yamamoto, M., Nomura, J., Ishihara, K., Takahara, H., Hibino, T., and Takeda, A. (2009). Neutral cysteine protease bleomycin hydrolase is essential for the breakdown of deiminated filaggrin into amino acids. *J. Biol. Chem.* *284*, 12829–12836.
35. Meyer-Hoffert, U. (2009). Reddish, scaly, and itchy: how proteases and their inhibitors contribute to inflammatory skin diseases. *Arch. Immunol. Ther. Exp. (Warsz.)* *57*, 345–354.
36. Matsui, T., Miyamoto, K., Kubo, A., Kawasaki, H., Ebihara, T., Hata, K., Tanahashi, S., Ichinose, S., Imoto, I., Inazawa, J., et al. (2011). *SASPase* regulates stratum corneum hydration through profilaggrin-to-filaggrin processing. *EMBO Mol Med* *3*, 320–333.
37. Vörner, H. (1901). Zur Kenntnis des Keratoma hereditarium palmare et plantare. *Arch. Dermatol. Syph.* *56*, 3–31.
38. Thost A. (1880). Über erbliche ichthyosis palmaris et plantaris cornea. (Med. Diss). Horning J., ed. Heidelberg.
39. Unna, P. (1883). Über das Keratoma palmare et plantare hereditarium, eine Studie zur Kerato-Nosologie. *Arch. Dermatol. Syph.* *15*, 231–270.
40. Greither, A. (1952). Keratosis extremitatum hereditaria progrediens mit dominantem Erbgang. *Hautarzt* *3*, 198–203.

41. Sybert, V.P., Dale, B.A., and Holbrook, K.A. (1988). Palmar-plantar keratoderma. A clinical, ultrastructural, and biochemical study. *J. Am. Acad. Dermatol.* *18*, 75–86.
42. Hatsell, S.J., Eady, R.A., Wennerstrand, L., Dopping-Hepenstal, P., Leigh, I.M., Munro, C., and Kelsell, D.P. (2001). Novel splice site mutation in keratin 1 underlies mild epidermolytic palmoplantar keratoderma in three kindreds. *J. Invest. Dermatol.* *116*, 606–609.
43. Reis, A., Hennies, H.C., Langbein, L., Digweed, M., Mischke, D., Drechsler, M., Schröck, E., Royer-Pokora, B., Franke, W.W., Sperling, K., et al. (1994). Keratin 9 gene mutations in epidermolytic palmoplantar keratoderma (EPPK). *Nat. Genet.* *6*, 174–179.
44. Küster, W., Reis, A., and Hennies, H.C. (2002). Epidermolytic palmoplantar keratoderma of Vörner: re-evaluation of Vörner's original family and identification of a novel keratin 9 mutation. *Arch. Dermatol. Res.* *294*, 268–272.
45. Kimonis, V., DiGiovanna, J.J., Yang, J.M., Doyle, S.Z., Bale, S.J., and Compton, J.G. (1994). A mutation in the V1 end domain of keratin 1 in non-epidermolytic palmar-plantar keratoderma. *J. Invest. Dermatol.* *103*, 764–769.
46. Gach, J.E., Munro, C.S., Lane, E.B., Wilson, N.J., and Moss, C. (2005). Two families with Greither's syndrome caused by a keratin 1 mutation. *J. Am. Acad. Dermatol.* *53(Suppl 1)*, S225–S230.
47. Covello, S.P., Irvine, A.D., McKenna, K.E., Munro, C.S., Nevin, N.C., Smith, F.J., Uitto, J., and McLean, W.H. (1998). Mutations in keratin K9 in kindreds with epidermolytic palmoplantar keratoderma and epidemiology in Northern Ireland. *J. Invest. Dermatol.* *111*, 1207–1209.
48. Hamm, H., Happle, R., Butterfass, T., and Traupe, H. (1988). Epidermolytic palmoplantar keratoderma of Vörner: is it the most frequent type of hereditary palmoplantar keratoderma? *Dermatologica* *177*, 138–145.
49. Küster, W., and Becker, A. (1992). Indication for the identity of palmoplantar keratoderma type Unna-Thost with type Vörner. Thost's family revisited 110 years later. *Acta Derm. Venereol.* *72*, 120–122.
50. Bouadjar, B., Benmazouzia, S., Prud'homme, J.F., Cure, S., and Fischer, J. (2000). Clinical and genetic studies of 3 large, consanguineous, Algerian families with Mal de Meleda. *Arch. Dermatol.* *136*, 1247–1252.

RESEARCH

Open Access

# Diverse spectrum of rare deafness genes underlies early-childhood hearing loss in Japanese patients: a cross-sectional, multi-center next-generation sequencing study

Hideki Mutai<sup>1†</sup>, Naohiro Suzuki<sup>1†</sup>, Atsushi Shimizu<sup>2</sup>, Chiharu Torii<sup>3</sup>, Kazunori Namba<sup>1</sup>, Noriko Morimoto<sup>4</sup>, Jun Kudoh<sup>5</sup>, Kimitaka Kaga<sup>6</sup>, Kenjiro Kosaki<sup>3</sup> and Tatsuo Matsunaga<sup>1\*</sup>

## Abstract

**Background:** Genetic tests for hereditary hearing loss inform clinical management of patients and can provide the first step in the development of therapeutics. However, comprehensive genetic tests for deafness genes by Sanger sequencing is extremely expensive and time-consuming. Next-generation sequencing (NGS) technology is advantageous for genetic diagnosis of heterogeneous diseases that involve numerous causative genes.

**Methods:** Genomic DNA samples from 58 subjects with hearing loss from 15 unrelated Japanese families were subjected to NGS to identify the genetic causes of hearing loss. Subjects did not have pathogenic *GJB2* mutations (the gene most often associated with inherited hearing loss), mitochondrial m.1555A>G or 3243A>G mutations, enlarged vestibular aqueduct, or auditory neuropathy. Clinical features of subjects were obtained from medical records. Genomic DNA was subjected to a custom-designed SureSelect Target Enrichment System to capture coding exons and proximal flanking intronic sequences of 84 genes responsible for nonsyndromic or syndromic hearing loss, and DNA was sequenced by Illumina GAllx (paired-end read). The sequences were mapped and quality-checked using the programs BWA, Novoalign, Picard, and GATK, and analyzed by Avadis NGS.

**Results:** Candidate genes were identified in 7 of the 15 families. These genes were *ACTG1*, *DFNA5*, *POU4F3*, *SLC26A5*, *SIX1*, *MYO7A*, *CDH23*, *PCDH15*, and *USH2A*, suggesting that a variety of genes underlie early-childhood hearing loss in Japanese patients. Mutations in Usher syndrome-related genes were detected in three families, including one double heterozygous mutation of *CDH23* and *PCDH15*.

**Conclusion:** Targeted NGS analysis revealed a diverse spectrum of rare deafness genes in Japanese subjects and underscores implications for efficient genetic testing.

**Keywords:** Hereditary hearing loss, Target gene capture, Deafness gene, Heterogeneity

## Background

Hearing loss is a common sensory defect, affecting approximately one in 500 to 1000 newborns [1]. Approximately 50% of congenital hearing loss cases and 70% of childhood hearing loss cases are attributed to genetic mutations [1]. The remaining 50% of congenital cases

are attributable to other factors such as prenatal exposure to measles, cytomegalovirus, premature birth, and newborn meningitis. Genetic tests for hereditary hearing loss assist in the clinical management of patients and can provide the first step in the development of therapeutics [2]. For example, early diagnosis of Usher syndrome, which comprises congenital hearing loss and late-onset retinitis pigmentosa, provides important information to choose communication modalities. However, causes of hereditary hearing loss are highly heterogeneous; more than 60 genes have been identified as responsible for nonsyndromic

\* Correspondence: matsunagatatsuo@kankakuki.go.jp

<sup>†</sup>Equal contributors

<sup>1</sup>Laboratory of Auditory Disorders, National Institute of Sensory Organs, National Hospital Organization Tokyo Medical Center, 2-5-1 Higashigaoka, Meguro, Tokyo 152-8902, Japan

Full list of author information is available at the end of the article





hearing loss [3], and several hundreds of syndromic diseases, such as Pendred syndrome and Usher syndrome, are accompanied by hearing loss. *GJB2* mutations are the most common cause of childhood hearing loss worldwide [1], followed by *SLC26A4* mutations [4]. *OTOF* mutations are common in patients with auditory neuropathy, which is characterized by normal outer hair cell function and abnormal neural conduction [5]. The prevalence of childhood hearing loss patients with mutations in other deafness-related genes is likely to be less than 1% [1]. Such high heterogeneity of hearing loss makes it impractical to perform genetic tests by Sanger sequencing. This is also the case for some types of syndromic hearing loss. For example, nine genes have been reported to cause Usher syndrome, and all are large and difficult to analyze using Sanger sequencing.

Next-generation sequencing (NGS) technology has been applied to genetic diagnosis of nonsyndromic hearing loss [6-8] and exploring the causes of hearing loss [9-11]. These studies have revealed that it is technically feasible to identify causative genes for nonsyndromic and syndromic hearing loss using targeted NGS [6,8]. In this study, we used targeted NGS to identify the genetic basis of hearing loss in Japanese families.

## Methods

### Subjects

This was a multi-center study of 58 subjects (36 subjects with hearing loss and 22 subjects with normal hearing) from 15 unrelated Japanese families in which at least two family members had bilateral hearing loss. All subjects were patients at the National Hospital Organization Tokyo Medical Center or a collaborating hospital. Medical histories were obtained and physical, audiological, and radiological examinations were carried out for the subjects and family members. Subjects with hearing loss related to environmental factors were excluded. Subjects with *GJB2* mutations or mitochondrial m.1555A>G or 3243A>G mutations were excluded. Subjects with enlarged vestibular aqueduct, which is often associated with *SLC26A4* mutations, and subjects with clinical features that suggested syndromic hearing loss were excluded. Subjects with auditory neuropathy were tested for *OTOF* mutations, which are associated with auditory neuropathy [12], and subjects with *OTOF* mutations were excluded. The Ethics Review Committees of the National Hospital Organization Tokyo Medical Center and all collaborating hospitals approved the study procedures. All procedures were conducted after written informed consent had been obtained from each subject or their parents.

### Targeted capture and DNA sequencing

We selected coding exons and proximal flanking intronic sequences of 84 genes, including 17 genes responsible for

autosomal dominant nonsyndromic hearing loss (DFNA), 32 genes responsible for autosomal recessive nonsyndromic hearing loss (DFNB), 8 genes responsible for both DFNA and DFNB, one gene responsible for auditory neuropathy, 3 genes responsible for X-linked hearing loss, and 23 genes responsible for syndromic hearing loss. A list of the targeted genes responsible for nonsyndromic or syndromic hearing loss is provided in the supporting material [Additional file 1]. More than 90% of the target genomic sequences were successfully designed to be captured by the SureSelect Target Enrichment System (Agilent Technologies, CA, USA) (data not shown). Genomic DNA was extracted from whole blood using the Genetra Puregene DNA isolation kit (QIAGEN, Hilden, Germany) and checked for quality using Qubit (Life technologies, CA, USA). Genomic DNA (3 µg) was fragmented into approximately 150 base pairs and used to capture the targeted genomic sequences. The captured DNA was subjected to the paired-end read sequencing system (GAIIx system; Illumina, CA, USA).

### Sequence analysis

Sequence analysis initially focused on the 61 genes responsible for nonsyndromic hearing loss. If no candidate mutations were detected among these genes, the 23 genes responsible for syndromic hearing loss were subjected to sequence analysis.

The sequences were mapped and quality-checked with the programs BWA, Novoalign, Picard, and GATK using the human reference sequence hg19/GRCh37. Single and multiple nucleotide variants, including small insertion or deletions that would affect amino acid sequences or could affect splice sites, were annotated by Avadis NGS v.1.4.5 (Strand Life Sciences, Bangalore, India). Variants already known as pathogenic mutations or detected with <1% frequency in public databases (dbSNP135 [13], 1000GENOME [14], NHLBI Exome Variant Server [15]) were extracted and further subjected to segregation analysis within each family. If no candidate variants were found, the 23 genes responsible for syndromic hearing loss were subjected to the same procedures.

Selected variants were classified as known mutations, possible pathogenic mutations, or variants with unknown pathogenicity; the latter classification was made if there were reports of a controversial finding of pathogenicity or >1% allele frequency in the in-house database of 95 (up to 189) Japanese subjects with normal hearing. Conservation of the corresponding mutated amino acid was compared across nine primate, 20 mammal, and 13 vertebrate species by UCSC Conservation [16]. Functional pathogenic effects of the variants were predicted by PolyPhen-2 [17] and PROVEAN [18]. Effect on splice-site mutations was predicted by NNSPLICE [19].

All the variants and their segregation in each family were confirmed by Sanger sequencing. The specific primer sets were selected from the resequencing amplicon probe sets (NCBI) or designed originally by Primer-BLAST (NCBI). The genotype of each individual and segregation in the family was characterized using DNA-SIS Pro (Hitachisoft, Tokyo, Japan).

### Structural modeling

To find sequences homologous to ACTG1 and MYO7A that could be used as the structural templates for the modeling exercise, we searched the Protein Data Bank (PDB) using Gapped BLAST [20] and PDBsum [21]. The crystal structure of *Limulus polyphemus* filamentous actin (PDB: 3B63) and the 4.1 protein-ezrin-radixin-moesin (FERM) domain of *Mus musculus* myosin VIIa in complex with Sans protein (PDB: 3PVL) were utilized as the templates to model ACTG1 with the p.G268S mutation and MYO7A with the p.W2160G mutation, respectively. The models were built using SWISS-MODEL [22-24] in

the automatic modeling mode and with default parameters. The quality of the models was evaluated using the Verify\_3D Structure Evaluation Server [25,26]. The  $\alpha$ -carbon frames and ribbon models were superimposed using Chimera [27].

### Results

Pedigrees of the seven families are shown in Figure 1; clinical features are described in Table 1 and supplemental materials [Additional file 2 and Additional file 3]. In this targeted NGS study, the mean read depth of the target regions was more than 100 $\times$  for all subjects (data not shown). Table 2 summarizes the number of variants detected from the 61 or 84 targeted genes for each subject. The number of variants was consistent across subjects (339–435 variants per subject for 61 genes, 539–607 variants per subject for 84 genes), which supported the reproducibility and reliability of our technical procedures and analytical pipeline. After excluding frequent variants (>1% in public databases, 12 variants of

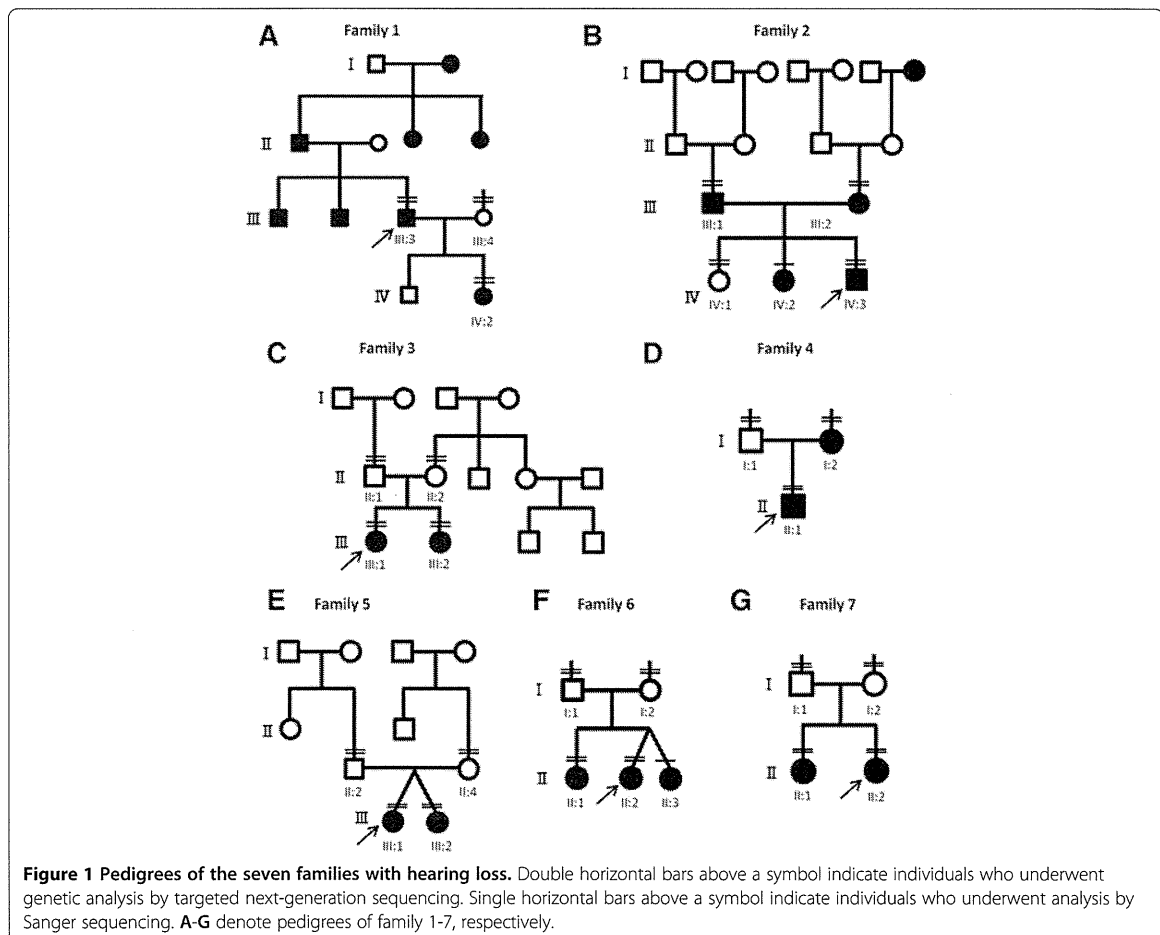


**Table 1 Summary of subjects with hearing loss**

Family	Subject	Age at onset (years)	Age at the time of the study (years)	Hearing loss severity (left/right)*	Progression
1	III:3	45	53	Moderate/Moderate	Yes
	IV:2	10	16	Mild/Normal	No
2	III:1	unknown	no data	Profound/Profound	Unknown
	III:2	unknown	no data	Moderate/Severe	Unknown
3	IV:3	0	1	Severe**	Yes
	III:1	0	9	Severe**	Unknown
4	III:2	0	6	Moderate/Moderate	Unknown
	I:2	0	30s	Profound/Profound	No
5	II:1	0	2	Profound/Profound	No
	III:1	0	2	Severe**	No
6	III:2	0	2	Profound**	No
	II:1	5	14	Profound/Severe	Yes
7	II:2	0	12	Profound/Profound	Yes
	II:1	0	3	Moderate (ASSR***)	Unknown
	II:2	0	0	Severe (ASSR)	Unknown

\*Hearing loss severity was evaluated based on average hearing level at 500, 1,000, 2,000, and 4,000 Hz (mild, 20–40 dB; moderate, 41–70 dB; severe, 71–95dB; profound, >95 dB) according to recommendations [3]. \*\*Binaural hearing level. \*\*\*ASSR, auditory steady state responses.

9 genes co-segregated with symptoms and were selected as possible pathogenic mutations (Table 3) or variants with uncertain pathogenicity in 7 families (Table 4).

#### Candidate mutations in each family

In family 1 (Figure 1A), subjects III:3 and IV:2 with hearing loss had a unique heterozygous missense mutation of *ACTG1* (c.802G >A; p.G268S), whereas subject III:4 with normal hearing did not. *ACTG1* encodes actin gamma 1 and is responsible for DFNA20/26 (OMIM 604717) [28]. The glycine residue at 268 of actin gamma 1 is located on a hydrophobic loop that has been suggested to be critical for polymerization of the actin monomers into a filament (Figures 2A and 2B) [29]. Molecular modeling predicted that the p.G268S mutation would disrupt the hydrophobic interactions that are important for polymerization of actin gamma 1 (Figures 2C and Figure 2D). The p.G268S mutant would weaken polymerization of actin gamma 1, which could result in destabilized cytoskeletal structure of stereocilia and dysfunction of the sensory hair cells.

Family 2 (Figure 1B) had two candidate genes with possible pathogenic mutations: A unique heterozygous *POU4F3* frameshift mutation, c.1007delC (p.A336Vfs), was detected in subjects III:1 and IV:3 with hearing loss, and a unique heterozygous *DFNA5* nonsense mutation, c.781C >T (p.R261X), was detected in subjects III:2 and IV:3 with hearing loss, whereas subject IV:1 with normal hearing had neither of these mutations. Sanger sequencing revealed that subject IV:2 with hearing loss had both the heterozygous mutations. *POU4F3* is responsible for DFNA15 (OMIM 602459) [30,31], and *DFNA5* is

responsible for DFNA5 (OMIM 600994) [32]. A frameshift mutation in *DFNA5*, which would lead to decreased expression, has been reported not to cause hearing loss [33]; therefore, the cause of hearing loss in subjects IV:2 and IV:3 is more likely to *POU4F3* with the p.A336Vfs mutation derived from subject III:1, rather than *DFNA5* with p.R261X mutation derived from subject III:2.

In family 3 (Figure 1C), subjects III:1 and III:2 with hearing loss had compound heterozygous *SLC26A5* with c.209G >A (p.W70X) and c.390A >C (p.R130S) mutations, whereas subjects II:1 and II:2 with normal hearing had a heterozygous p.W70X mutation and a heterozygous p.R130S mutation, respectively. *SLC26A5* encodes prestin, a member of the SLC26A/SulP transporter family, and is responsible for DFNB61 (OMIM 613865) [34].

In family 4 (Figure 1D), subjects I:2 and II:1 with hearing loss did not have candidate mutations in the first 61 genes. Analysis of the additional 23 genes indicated a heterozygous *SIX1* mutation, c.328C >T (p.R110W), in the subjects with hearing loss but not in subject I:1 with normal hearing. *SIX1* is responsible for DFNA23 (OMIM 605192) and Branchio-otic syndrome 3 (BOS3, OMIM 608389). The p.R110W mutation was previously reported in two BOS3 families [35]. To make the clinical diagnosis of branchiootorenal syndrome or branchiootic syndrome, major and minor criteria of these syndromes must be present [36]. In the affected subjects of the present study, clinical histories were thoroughly evaluated and physical examination of the ear, nose, throat, head and neck, and audiological tests were performed. In addition, CT of the temporal bone was evaluated in subject II:1. With these examinations, the affected subjects did not

**Table 2 Summary of the number of variants detected in each subject**

Family	Subject	Number of genes analyzed	No.SNV/MNV*	No. non-synonymous SNV/MNV
1	III:3	61	414	84
	III:4	61	370	74
	IV:2	61	391	82
2	III:1	61	386	81
	III:2	61	422	87
	IV:1	61	435	82
3	IV:3	61	400	84
	II:1	61	383	82
	II:2	61	339	70
4	III:1	61	350	74
	III:2	61	398	86
	I:1	84	570	138
5	I:2	84	569	126
	II:1	84	546	131
	II:2	61	388	72
6	II:4	61	374	87
	III:1	61	361	84
	III:2	61	396	85
7	I:1	61	429	96
	I:2	61	371	81
	II:1	61	378	86
8	II:2	61	375	84
	I:1	84	607	139
	I:2	84	554	126
9	II:2	84	582	132
	II:1	84	539	117

\*SNV, single nucleotide variant; MNV, multiple nucleotide variant.

present clinical features of the major and minor criteria other than hearing loss. Therefore, family 4 was considered to have non-syndromic hearing loss, DFNA23, based on the clinical information available at the time of this study.

In family 5 (Figure 1E), subjects III:1 and III:2 with hearing loss had compound heterozygous *MYO7A* mutations, c.6439-2A >G (intron 51) and c.6478T >G (p.W2160G). Subjects II:2 and II:4 with normal hearing had a heterozygous c.6439-2A >G mutation and a heterozygous p.W2160G mutation, respectively. *MYO7A* is responsible for DFNA11 (OMIM 601317) [37], DFNB2 (OMIM 600060) [38], and Usher syndrome 1B (OMIM 276900) [39]. Tryptophan 2160 in myosin 7A was found to be located in a carboxyl-terminal FERM domain in the myosin-tail (Figures 3A and Figure 3B); this domain reportedly associates with filamentous actin [40] and contributes to hair bundle formation. Molecular modeling predicted that the p.W2160G mutation would reduce hydrophobic interactions among residues in the center of

the F3 subdomain of the FERM domain (Figures 3C and 3D). The p.W2160G mutation would destabilize the structure of the F3 domain and could result in disrupted protein interaction and stereocilia degeneration of the sensory hair cells [41,42].

In family 6 (Figure 1F), subjects II:1 and II:2 with hearing loss had a heterozygous *CDH23* mutation, c.719C>T (p.P240L), and a heterozygous *PCDH15* mutation, c.848G >A (p.R283H). Sanger sequencing revealed that the other subject with hearing loss (subject II:3) also had both heterozygous *CDH23* and *PCDH15* mutations. A p.P240L mutation in *CDH23* has been reported to be pathogenic [43]. Subject I:1 with normal hearing had a heterozygous mutation in *CDH23* (p.P240L), and subject I:2 with normal hearing had a heterozygous mutation in *PCDH15* (p.R283H). *CDH23* is responsible for both DFNB12 (OMIM 601386) and Usher syndrome 1D (OMIM 601067) [44], whereas *PCDH15* is responsible for both DFNB23 (OMIM 609533) and Usher syndrome 1F (OMIM 602083) [45]. Double heterozygous mutations of *CDH23*